# The N-Terminal Basic Domain of the HIV-1 Matrix Protein Does Not Contain a Conventional Nuclear Localization Sequence But Is Required for DNA Binding and Protein Self-Association†

Anna C. Hearps,‡ Kylie M. Wagstaff,‡ Sabine C. Piller,§ and David A. Jans*,‡

*Nuclear Signalling Laboratory, Department of Biochemistry and Molecular Biology, Monash University, Clayton, Victoria 3800, and Centre for Virus Research, Westmead Millennium Institute, P.O. Box 412, Westmead, New South Wales 2145, Australia*

*Received July 10, 2007; Revised Manuscript Received November 1, 2007*

ABSTRACT: The HIV p17 or matrix (MA) protein has long been implicated in the process of nuclear import of the HIV genome and thus the ability of the virus to infect nondividing cells such as macrophages. While it has been demonstrated that MA is not absolutely required for this process, debate continues to surround the subcellular targeting properties of MA and its potential contribution to nuclear import of the HIV cDNA. Through the use of in vitro techniques we have determined that, despite the ability of MA to interact with importins, the full-length protein fails to enter the nucleus of cells. While MA does contain a region of basic amino acids within its N-terminus which can confer nuclear accumulation of a fusion protein, we show that this is due to nuclear retention mediated by DNA binding and does not represent facilitated import. Importantly, we show that the $^{26}$KK residues of MA, previously thought to be part of a nuclear localization sequence, are absolutely required for a number of MA's functions including its ability to bind DNA and RNA and its propensity to form high-order multimers/protein aggregates. The results presented here indicate that the N-terminal basic domain of MA does not appear likely to play a role in HIV cDNA nuclear import; rather this region appears to be a crucial structural and functional motif whose integrity is required for a number of other roles performed by MA during viral infection.

The HIV MA[1] protein is a multifunctional protein that serves a structural role within the HIV virion and is also responsible for mediating the assembly and release of viral particles (reviewed in ref *1*). Early in infection, MA is found within a complex known as the preintegration complex (PIC) with the newly synthesized viral cDNA and other viral proteins including reverse transcriptase, integrase (IN), and Vpr (*2*, *3*). HIV is able to infect nondividing cells such as macrophages (*4*), which is thought to be important for the long-term pathogenicity of HIV/AIDS. Infection of nondividing cells requires the HIV PIC to penetrate an intact nuclear envelope, and despite extensive analyses of the import properties of the individual PIC components, the mechanism of PIC nuclear import remains highly controversial (reviewed in ref *5*).

Nuclear import of molecules larger than 40−45 kDa is a tightly regulated process controlled by a superfamily of proteins known as importins (Imp's). Cargoes destined for the nucleus typically contain a stretch of basic amino acids known as a nuclear localization sequence (NLS) which is recognized either directly by the Imp $\beta$ import receptor, or one of the many homologues thereof, or via the adapter protein Imp $\alpha$ as part of an Imp $\alpha/\beta$ heterodimer. Imp $\beta$ is thought to form transient interactions with the proteins which line the nuclear pores (nucleoporins), resulting in the translocation of the import cargo−Imp complex through the pore and into the nucleus (*6*). Within the nucleus, the binding of Ran in its GTP-bound form to Imp $\beta$ stimulates dissociation of the complex and release of the import cargo. Protein nuclear export occurs in an analogous fashion, with export cargo containing a nuclear export sequence (NES) being recognized and bound by an exportin such as Crm1, which traverses the nuclear pore and is dissociated in the cytoplasm by the binding of Ran in its GDP-bound state (see refs *7*−*9* for review).

As mentioned, the method utilized by HIV to translocate its genome through the nuclear envelope of a nondividing cell remains highly controversial (reviewed in refs *10* and *11*). MA was initially implicated in PIC nuclear import due to the identification of a putative, basic-type NLS within amino acids (aa's) 25−33 which was found to be able to direct nuclear import of a large fusion protein (*12*, *13*). The potential of MA as a nucleophilic protein was supported by the observation that the MA NLS interacted with a key member of the nuclear import pathway, Imp $\alpha$ (*13*−*15*). Although originally thought to constitute a crucial determi-

† We acknowledge the support of the National Health and Research Council, Australia (Fellowship Nos. 143790 and 333013 and Project Grant Nos. 143710 and 22274).

* To whom correspondence should be addressed. Phone: +613 9905 3778. Fax: +613 9905 3726. E-mail: David.Jans@med.monash.edu.au.

‡ Monash University.

§ Westmead Millennium Institute.

[1] Abbreviations: CSLM, confocal laser scanning microscopy; DTAF, 5-(4,6-dichlorotriazinyl)aminofluorescein, GFP, green fluorescent protein; GST, glutathione S-transferase, HIV, human immunodeficiency virus; Imp, importin; IN, integrase; LMB, leptomycin B; MA, matrix protein; NES, nuclear export signal; NLS, nuclear localization signal; PIC, preintegration complex; Tag, simian virus 40 large tumor antigen; WT, wild type.

10.1021/bi701360j CCC: $40.75 
Published on Web 01/29/2008

nant of PIC nuclear import (*12*, *16*), many subsequent studies have demonstrated that the MA NLS is not essential for HIV infection of nondividing cells (*17*−*21*). Other potential nucleophilic proteins such as the Vpr protein (*19*), regions within IN (*22*−*24*), and the cDNA flap (*24*−*26*) have similarly been suggested as crucial determinants of HIV nuclear import and subsequently shown not to be essential for this process, suggesting that the HIV PIC may contain multiple, redundant nuclear import signals (*5*) (see however ref *27*). Whether MA represents one of these signals and what contribution, if any, it makes to the process of HIV cDNA nuclear import remain unclear.

While MA is purported to contain an NLS within its N-terminus, subcellular localization studies using the full-length protein have shown it to be excluded from the nucleus (*18*, *20*, *28*, *29*). The suggestion that MA may contain a dominant, Crm1-recognized NES appeared to reconcile this anomaly (*30*), but subsequent studies do not support this idea (*29*). The precise location and nature of the targeting signals responsible for the cytoplasmic localization of MA under steady-state conditions remain unclear.

Attempts to investigate the nucleophilic properties of MA in vivo have been problematic due to the multifunctional nature of this protein (reviewed in ref *31*) and the high degree of redundancy which appears to exist within HIV. Although mutagenesis of the MA NLS has been used as a tool to investigate its role in PIC nuclear import, such studies are confounded by the involvement of this region in a number of unrelated processes including viral assembly (*32*, *33*), plasma membrane binding (*34*, *35*), and polyprotein processing (*18*, *36*). One of the advantages of investigating the cellular targeting signals of proteins such as MA in vitro is that nuclear transport can be examined specifically in isolation from these other complicating processes.

In this study, we have used various approaches to thoroughly assess the nuclear import properties of MA, confirming that despite its ability to interact with Imp's in vitro, MA fails to enter the nucleus of cells in either an in vitro transport assay or transfected cells. Through the use of truncated MA derivatives we demonstrate that the N-terminal basic region can indeed confer nuclear accumulation, but via DNA binding rather than through Imp-mediated nuclear import. The $^{26}$KK residues of MA appear to be critical for many of MA's properties including Imp binding and protein aggregation and are absolutely required for the ability of MA to interact with both DNA and RNA. This suggests that the purported NLS within MA does not represent a conventional nucleophilic sequence but rather is part of a key structural motif required for a number of MA's functions.

## MATERIALS AND METHODS

*Plasmids*. MA-containing constructs for transfection and protein expression were created using the Gateway cloning technology (Invitrogen). DNA fragments encoding MA residues 2−132 were generated via PCR using the pNL4-3 proviral clone (NIH AIDS Reagent Reference Program No. 114) as the template and incorporating attB1 and attB2 sites into the N- and C-termini, respectively. This enabled the initial incorporation of the fragment into the pDONR207 vector (Invitrogen) via a BP reaction and subsequent recombination into the appropriate DEST vector via an LR reaction according to the manufacturer's recommendations. DEST vectors utilized for transfection experiments included pEpiDESTC (*37*) (expressing GFP-tagged protein) and pcLumioDEST (expressing V5-tagged protein, Invitrogen). The DEST vectors pRfA−GFP−DEST (expressing His-tagged MA−GFP) and pEXP3 (expressing His−V5-tagged protein, Invitrogen) were used for the expression of recombinant MA proteins. PCR products destined for constructs containing N-terminal fusions were engineered to contain a stop codon after aa 132. The N-terminal Met codon was omitted from all constructs to prevent internal priming.

The GFP−Rev(2−116) encoding construct, used as a control within transfection experiments, has been described previously (*38*).

*Cells and Transfections*. HeLa human cervical cancer, Cos-7 green African monkey kidney, and HTC rat hepatoma tissue culture cell lines were maintained at 37 °C in DMEM supplemented with 10% FCS, L-glutamine, penicillin, and streptomycin in a humidified incubator with 5% $CO_2$. For in vitro transport assay experiments, HTC cells were seeded onto glass coverslips 2 days prior to use to achieve a confluency of 70% at the time of experimentation. For transfection experiments, the cells were seeded onto coverslips 1 day prior to transfection. The cells were typically transfected at a confluency of 60−80% with 2 $\mu$g of plasmid DNA per coverslip using Lipofectamine 2000 (Invitrogen) according to the manufacturer's instructions. Following transfection, the cells were maintained in media containing 5% FCS and imaged live using confocal laser scanning microscopy (CLSM) 16−24 h post-transfection. In some experiments, Crm1-mediated nuclear export was blocked via the addition of 5 $\mu$M leptomycin B (LMB) 6 h prior to imaging. Nonfluorescently tagged MA constructs were visualized using immunofluorescent labeling. Briefly, the cells were fixed using 4% paraformaldehyde, blocked in blocking buffer (PBS containing 3% BSA), and permeabilized with blocking buffer containing 0.2% Triton-X 100 and the proteins visualized using either monoclonal anti-V5 antibody (Invitrogen) or rabbit MA antiserum (NIH AIDS Reagent Reference Program No. 4811) and the appropriate Alexa 486-conjugated secondary antibody (Molecular Probes).

*Expression and Purification of Recombinant Protein*. For expression of recombinant $His_6$-tagged MA proteins, plasmids were transformed into M15 bacteria, grown to an $OD_{600}$ of approximately 1.0, and induced with 1 mM IPTG for 16 h at 28 °C. Protein was purified from bacterial pellets under native conditions. Briefly, bacterial pellets were resuspended in native buffer (50 mM $NaH_2PO_4$, 300 mM NaCl, pH 8.0) containing 10 mM imidazole and lysed with 3 mg/mL lysozyme on ice for 30 min in the presence of 1 U/mL DNAse and Complete EDTA-free protease inhibitors (Roche). Insoluble material was pelleted at 11000*g* for 1 h at 4 °C and the supernatant incubated with 4 mL of pre-equilibrated $Ni^+$−NTA bead slurry (Qiagen) for 1 h at 4 °C. The beads were washed and the protein was subsequently eluted in the above buffer containing 20 and 500 mM imidazole, respectively. Imidazole was removed via dialysis against native buffer and the protein concentrated in VivaSpin concentrators (Millipore). The final protein concentration was determined using a dye binding assay (BioRad).

GST-tagged mouse Imp proteins and the GFP-tagged peptide containing the simian virus SV40 large tumor antigen

(Tag) NLS (aa's 111−135) were expressed and purified as previously described (refs *39* and *40*, respectively). The expression, purification, and labeling of the HIV-1 IN protein with the fluorescent dye DTAF has been described previously (*41*).

*In Vitro Nuclear Transport Assay*. Nuclear import of fluorescently labeled MA was investigated in vitro using mechanically perforated HTC cells as previously described (*42*). Briefly, perforation was used to remove the plasma membrane of the cells, but leave the nuclear membrane intact, and the perforated cells were then inverted onto a microscope slide over a chamber containing rabbit reticulocyte lysate (30 $\mu$g/mL, Promega), an ATP regenerating system (0.125 mg/mL creatine phosphokinase, 30 mM creatine phosphate, 2 mM ATP), 70 kDa Texas Red-conjugated dextran (to assess nuclear integrity), 5 $\mu$M GFP-tagged MA protein (or appropriate control protein), and IB buffer (110 mM KCl, 5 mM $NaHCO_3$, 5 mM $MgCl_2$, 1 mM EGTA, 0.1 mM $CaCl_2$, 20 mM Hepes, 1 mM DTT, pH 7.4) in a final volume of 5 $\mu$L. Where required, 0.025% CHAPS (a detergent used to permeabilize the nuclear membrane (*43*)) was added to estimate the extent to which MA proteins may accumulate in the nucleus due to binding to nuclear components.

*ALPHAScreen Assay*. The interaction of MA−GFP (both WT and mutant) with Imp proteins was determined using an established ALPHAScreen assay (*44*). A 60 nM concentration of $His_6$-tagged MA−GFP was bound to $Ni^{2+}$ chelate acceptor beads and incubated with increasing concentrations of biotinylated GST-tagged Imp's (or GST alone) bound to streptavidin-coated donor beads. To detect binding to the Imp $\alpha/\beta$ complex, biotinylated Imp $\alpha$ was first predimerized to nonbiotinylated Imp $\beta$ at a concentration of 13.6 $\mu$M at 24 °C for 15 min in IB buffer. Binding interactions were detected using a FUSION$\alpha$ (Perkin-Elmer) plate reader. The interaction of the control protein GFP−Tag NLS with Imp $\alpha$ was determined under similar conditions.

*DNA and RNA Gel Shift Assays*. The interaction of WT and $^{26}$KK−TT-mutated MA−GFP proteins (plus truncated versions thereof) with DNA was assessed using an electrophoretic gel mobility shift assay. A 250 ng sample of linearized plasmid DNA was preincubated with increasing concentrations of MA−GFP protein for 10 min at 24 °C. The complexes were resolved on an 0.8% agarose gel at 4 °C, and the DNA was visualized via ethidium bromide staining. For competition experiments, MA−GFP was preincubated with either Imp $\beta$−GST or GST alone for 10 min at 24 °C prior to the addition of DNA.

The interaction of His−V5-tagged WT and $^{26}$KK−TT-mutated MA with RNA was also determined via a gel electrophoresis assay. Total RNA was extracted from HeLa cells using TRIzol (Invitrogen) according to the manufacturer's recommendations. The integrity of isolated RNA was confirmed using a denaturing formaldehyde agarose gel. RNA was incubated with increasing concentrations of either WT or $^{26}$KK−TT-mutant His-V5−MA protein (together with a GST negative control) for 10 min at room temperature, and the complexes were resolved on an agarose gel as above.

*Sedimentation Analysis*. Ultracentrifugation was used to determine the propensity of both GFP-tagged WT and $^{26}$KK−TT-mutant MA derivatives to form protein aggregates. A 10 $\mu$M concentration of GFP-tagged MA protein, or GFP alone, was precleared of aggregated material at 16000*g* for 15 min at 24 °C before centrifugation at 100000*g* for 1 h at 24 °C. The ability of MA to form aggregates in the presence of Imp's was determined by preincubating MA−GFP protein with a 10 $\mu$M concentration of GST−Imp $\alpha$/Rch1, GST−Imp $\beta$, or GST alone prior to ultracentrifugation. The supernatants were removed and the pellets washed once with PBS and resuspended in 1× SDS loading buffer. The protein composition of equivalent volumes of supernatant and pellet fractions was analyzed via SDS−PAGE and Western blotting using antibodies to GFP (Roche).

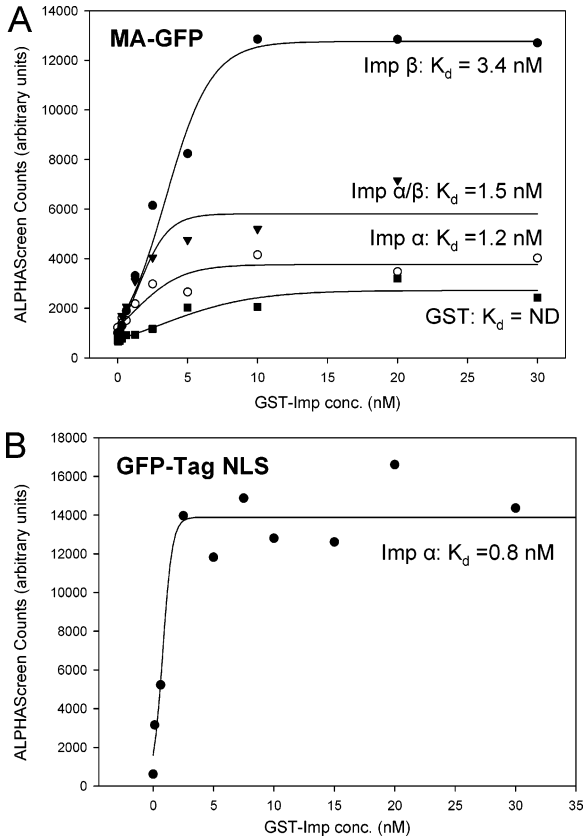


FIGURE 1: MA−GFP interacts with Imp $\beta$ and Imp $\alpha/\beta$ but not Imp $\alpha$. (A) MA−GFP was incubated with increasing concentrations of biotinylated GST−Imp $\alpha$ (Rch1; open circles), GST−Imp $\beta$1 (filled circles), predimerized GST−Imp $\alpha/\beta$ (triangles), or GST alone (squares) and an ALPHAScreen assay performed to determine the binding affinity as described in the Materials and Methods. The interaction of the control protein GFP−Tag NLS with Imp $\alpha$ (B) was determined under conditions similar to those in (A). Sigmoidal curves were fitted using the SigmaPlot software to determine the apparent dissociation constants ($K_d$, nM) as indicated. Each point represents the average of triplicate results from a single representative experiment. GFP alone exhibits no significant interaction with Imp's within this assay (*44*; data not shown). ND = $K_d$ value not determined due to low binding affinity.

## RESULTS

*MA Interacts with Imp $\beta$ and Imp $\alpha/\beta$ but Not with Imp $\alpha$*. As a first step in investigating the nucleophilic potential of MA, we tested whether MA could interact with members of the Imp family of nuclear importing proteins using an established ALPHAScreen assay (*44*). Figure 1A shows results from one representative experiment and indicates that a bacterially expressed MA−GFP fusion protein interacts with Imp $\beta$ and also Imp $\alpha/\beta$, with average $K_d$ values ($\pm$SEM) of 3.9 $\pm$ 0.2 and 1.2 $\pm$ 0.2 nM, respectively (see Table 1). However, the interaction of MA−GFP with Imp

Table 1: Average Binding Affinities ($K_d$) and Maximal Binding ($B_{max}$) of MA−GFP to Imp's[a]

| | $K_d$ (nM) ± SEM | $B_{max}$[b] ± SEM |
|---|---|---|
| GST−Imp α | ND | 3420 ± 320 |
| GST−Imp α/β | 1.2 ± 0.2 | 6700 ± 1300 |
| GST−Imp β | 3.9 ± 0.2 | 12150 ± 2090 |
| GST | ND | 3030 ± 215 |

[a] As determined by an ALPHAScreen assay (Figure 1, $n = 5$). ND = not determined. [b] $B_{max}$ values shown are in ALPHAScreen counts (arbitrary units).

α was not markedly greater than that observed for GST alone. This is highlighted by the observation that the average maximal bindings for Imp α and GST alone were 3420 ± 320 and 3030 ± 215 (arbitrary units), respectively, compared to values of 12150 ± 2090 and 6700 ± 1300 for Imp β and Imp α/β, respectively (Table 1). A similar Imp binding profile was observed for MA−GFP and indeed GFP−MA (GFP fused to the N-terminus of MA) as well using native gel electrophoresis (data not shown). These results suggest that MA interacts with both Imp β and the Imp α/β complex with high affinity, but does not exhibit a substantial interaction with Imp α alone. That Imp α was fully functional within this assay was confirmed by its interaction with the control protein GFP−Tag NLS (Figure 1B, $K_d$ of 0.8 nM).

*MA Is Excluded from the Nucleus of Transfected Cells.* To determine the subcellular localization of MA, cells were transfected with plasmid constructs encoding either GFP−MA or GFP alone and imaged live using CLSM. GFP contains no specific targeting signals and is small enough (molecular mass of around 27 kDa) to diffuse through the nuclear pore. Figure 2 shows that while GFP alone is evenly distributed throughout both the cytoplasm and the nucleus, GFP−MA is excluded from the nucleus of the cells and is almost completely restricted to the cytoplasm, as indicated by the $F_n/F_c$ of around 0.25 compared to a value of 1.5 for GFP alone (Figure 2A,B). As the size of the GFP−MA fusion protein (46 kDa) is just above the 40−45 kDa cutoff for passive diffusion of proteins into the nucleus, it is possible that GFP−MA may be excluded from the nucleus due to its size. To investigate this more closely, an alternate V5 epitope-tagged transfection construct was created which has a total molecular mass of around 18 kDa. V5−MA protein was transfected into the cells and the protein distribution visualized via immunofluorescence. Like GFP−MA, V5−MA was also found to be excluded from the nucleus, with an $F_n/F_c$ of approximately 0.3 (Figure 2A,B). The subcellular distribution of MA was not influenced by the location of the epitope tag, as transfection of an MA−V5 construct (V5 fused to the C-terminus of MA) showed a similar degree of nuclear exclusion (data not shown). Within infected cells, MA is normally cotranslationally myristoylated at the $Gly^2$ position, which can modulate its structural and functional properties (see ref *31* for review). In contrast to N-terminally tagged MA proteins, the N-terminus of the MA−V5 construct is accessible for myristoylation, yet is also excluded from the nucleus. This suggests that the lack of nuclear accumulation of N-terminally tagged MA is unlikely to be attributable to its inability to be myristoylated.

In the absence of a specific targeting signal, a protein with a molecular mass of only 18 kDa would normally show diffuse localization throughout the cytoplasmic and nuclear

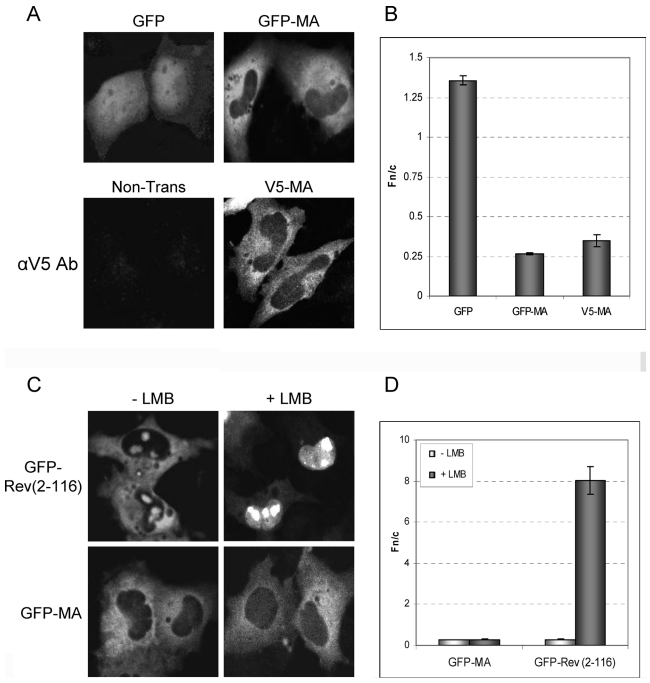


FIGURE 2: GFP−MA and V5−MA are excluded from the nucleus of transfected cells. (A) Cos-7 cells were transfected to express GFP alone (upper left panel) or GFP−MA (upper right panel) and imaged live using CLSM 16 h post-transfection. Untransfected Cos-7 cells (lower left panel) or cells transfected to express V5−MA (lower right panel) were fixed, immunostained with anti-V5 antibody, and imaged using CLSM. (B) Image analysis was performed on CLSM images such as those in (A) using ImageJ (NIH) software. All values used were within the linear fluorescence range. The nuclear to cytoplasmic fluorescence ratio ($F_n/F_c$) was calculated using the equation $F_n/F_c = (F_n - F_b)/(F_c - F_b)$, where $F_n$, $F_b$, and $F_c$ represent the nuclear, background, and cytoplasmic fluorescence, respectively. The values represent the mean $F_n/F_c$ ± SEM ($n \geq 30$) from a single experiment representative of at least four experiments. (C) Typical CLSM images of Cos-7 cells transfected to express GFP−Rev(2−116) (upper panels) or GFP−MA (lower panels) which were untreated (left panels) or treated with 5 μM LMB 6 h prior to live imaging (right panels). (D) Images such as those in (C) were analyzed as described in (B). The values represent the mean $F_n/F_c$ ± SEM ($n \geq 30$) from a single experiment representative of four experiments. Similar results were observed in both HeLa and 293-T cells (not shown).

compartments. One theory proposed to explain the observed nuclear exclusion of MA was that the protein is actively exported from the nucleus (*30*). To determine whether MA was subject to Crm1-mediated nuclear export, cells transfected to express GFP−MA were treated with leptomycin B (LMB), a potent inhibitor of the exportin Crm1, which is the predominant mediator of nuclear export within the cell. The HIV Rev protein is exported from the nucleus by Crm1 (*45*) and was used as a positive control in these experiments. The addition of LMB to cells transfected to express GFP−Rev(2−116) dramatically increased its nuclear accumulation (Figure 2C,D), confirming the efficacy of the LMB treatment. In contrast, the addition of LMB to cells expressing GFP−MA (Figure 2C,D), V5−MA, or MA−V5 (data not shown) had no effect on the localization of MA. These results indicate that Crm1-mediated nuclear export is not responsible for the nuclear exclusion of MA observed within transfected cells; whether this may also be the case within infected cells where other viral proteins may interact with MA remains to be determined.

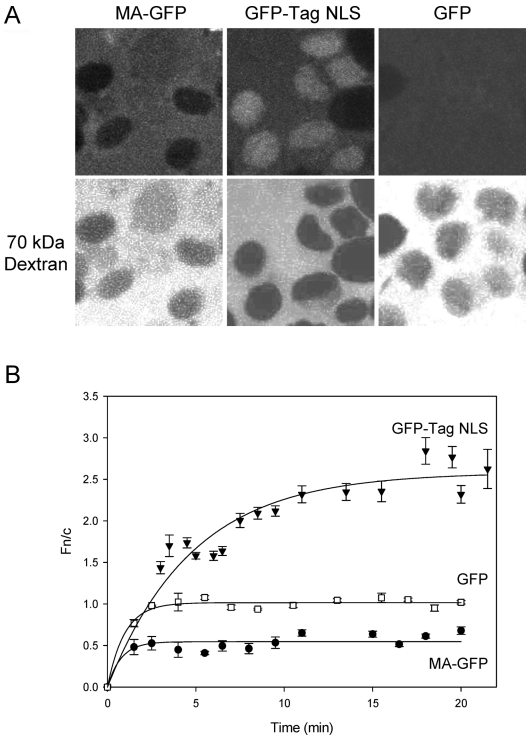


FIGURE 3: MA−GFP fails to enter the nucleus of semi-intact cells in vitro. Nuclear import of MA−GFP was reconstituted in vitro in mechanically perforated HTC cells in the presence of exogenous cytosol and an ATP-regenerating system as described in the Materials and Methods. (A) CLSM images were acquired periodically for accumulation of MA−GFP (left panel), the control protein GFP−Tag NLS (center panel), or GFP alone (right panel) into intact nuclei. Nuclear integrity was determined by the exclusion of a Texas Red-labeled 70 kDa dextran (lower panel). (B) Image analysis was performed on CLSM images such as those in (A) as described in the caption to Figure 2. Nuclear import kinetics were plotted using SigmaPlot software and exponential curves fitted for MA−GFP (circles), GFP−Tag NLS (triangles), and GFP (squares) as indicated. Each point represents the mean $F_n/F_c \pm$ SEM ($n \geq 5$).

*MA Fails To Enter the Nucleus of Cells in Vitro.* To confirm that MA does not possess nuclear import potential, we analyzed the localization of recombinant MA−GFP protein in vitro using a mechanically perforated HTC cell system where the nuclear accumulation of fluorescent protein within unfixed cells is monitored over time using CLSM. The GFP-tagged SV40 Tag NLS contains a potent Imp $\alpha/\beta$-recognized nuclear targeting motif and exhibits rapid nuclear accumulation within this system (Figure 3). Consistent with the results observed in transfected cells, MA−GFP was unable to enter the nucleus of perforated cells (Figure 3), confirming that MA lacks nucleophilic potential. GFP−MA exhibited a similar degree of nuclear exclusion within this assay (data not shown), suggesting that the location of the fluorescent tag did not influence MA's import properties.

*The N-Terminal Region of MA Can Confer Nuclear Accumulation in Transfected Cells.* Having established that Crm1-mediated nuclear export is not responsible for the observed nuclear exclusion of MA, we concluded that some other mechanism was operating to retain MA in the cytoplasm. We postulated that MA may bind to a cytosolic component, which would prevent its diffusion into the nucleus, or alternatively that MA may be multimerizing and thus be prevented from diffusing into the nucleus due to the large size of a potential MA multimer. To attempt to map possible retention signals/binding sites within MA, we created a number of MA truncations (Figure 4A).

The first 33 aa's of MA contain a high number of basic residues (10 or 11, depending on the strain) and include the purported basic-type NLS. To investigate the function of this region, we created a construct containing this region alone (aa's 2−33) and one lacking this region (aa's 34−132). A third truncation containing the globular head domain (aa's 2−104) and lacking the C-terminal region was also created to assess the influence of the unstructured C-terminal region on MA's subcellular localization (see Figure 4A).

Transfection of GFP-tagged MA truncations or full-length MA ($MA_{FL}$) into cells revealed that the N-terminal basic region of MA confers accumulation of the fusion protein within the nucleus (Figure 4B, upper panel). In contrast, $MA_{2-104}$ was excluded from the nucleus in a fashion similar to that of $MA_{FL}$ while $MA_{34-132}$ showed a distribution comparable to that of GFP alone. The degree of nuclear accumulation or exclusion seen with each truncation was quantitated (Figure 4C), the results confirming that $MA_{2-33}$ does indeed concentrate in the nucleus of cells with an $F_n/F_c$ of approximately 2.2, while $MA_{FL}$ and $MA_{2-104}$ both show nuclear exclusion ($F_n/F_c$ of around 0.3), and the distribution of $MA_{34-132}$ is similar to that of GFP alone ($F_n/F_c$ of 1.4 for both). These results imply that while MA may possess a weak nuclear import/retention signal within its N-terminus, regions within aa's 2−104 of MA confer exclusion from the nucleus, which within the context of the full-length protein constitute the predominant targeting signal within MA.

*Mutation of the $^{26}$KK Residues within MA Abolishes Both Its Nuclear and Its Cytoplasmic Retention.* Having established that $MA_{2-33}$ can confer accumulation within the nucleus, we explored whether this was due to the action of the purported NLS, which is located between residues 25 and 33. To investigate the involvement of this region in the cellular localization of MA, we used site-directed mutagenesis to create a $^{26}$KK to TT mutation within the $MA_{2-33}$, $MA_{2-104}$, and $MA_{FL}$ constructs. Transfection of constructs encoding the GFP−MA mutants revealed that mutation of the proposed NLS did in fact abolish the nuclear accumulation conferred by $MA_{2-33}$ (Figure 4B, lower panel). However, this mutation also eliminated the cytoplasmic retention conferred by both the FL and 2−104 proteins, with the $^{26}$KK−TT-mutant derivatives showing diffuse localization between both the nucleus and the cytoplasm, similar to that of GFP alone (Figure 4B,C). Western blotting of transfected cell lysates confirmed the expression of the intact fusion proteins (data not shown). These results suggest that the $^{26}$KK residues represent a crucial structural and/or functional domain whose integrity is essential for not only the nuclear localization of the N-terminal region but also the cytoplasmic retention of other regions of MA.

*The N-Terminal Region of MA Is Retained in the Nucleus via Interaction with Nuclear Component(s).* The relatively small size of GFP−$MA_{2-33}$ (31 kDa) means that its nuclear accumulation could result from diffusion of the protein through the nuclear pore and retention within the nucleus via interaction with a nuclear component. To investigate this possibility, we utilized our in vitro transport assay to assess the nuclear accumulation of the $MA_{2-33}$ truncation in the absence of an intact nuclear envelope. The addition of recombinant $MA_{2-33}$−GFP protein to intact nuclei resulted

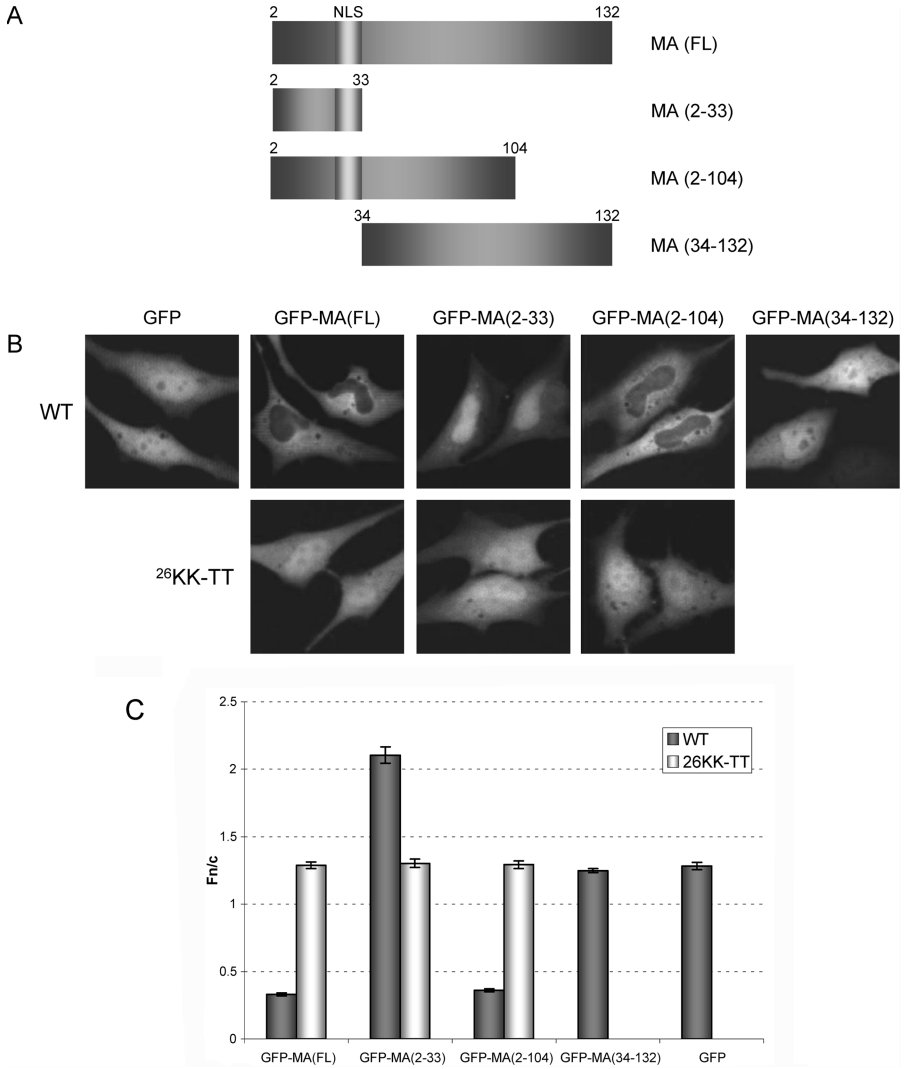


FIGURE 4: The $^{26}$KK−TT mutation within MA abolishes the nuclear localization of GFP−$MA_{2-33}$ and the cytoplasmic localization of GFP−$MA_{FL}$ and GFP−$MA_{2-104}$. (A) Schematic of the various MA truncations constructed with the location of the purported NLS indicated. (B) HeLa cells were transfected to express the indicated MA proteins fused to GFP (outlined in (A)) together with the corresponding mutant containing a $^{26}$KK−TT substitution as indicated. Representative CLSM images of cells transfected with either WT (upper panel) or $^{26}$KK−TT-mutant (lower panel) MA constructs are shown (GFP-expressing cells are included for comparison). (C) Images such as those in (B) were analyzed as described in the caption to Figure 2. The values represent the mean $F_n/F_c \pm$ SEM ($n \geq 35$) from a single representative experiment. Similar results were observed in Cos-7 cells (not shown).

in nuclear accumulation with an $F_n/F_c$ of 1.5 (Figure 5B,C), which, although not as high as that observed with the potent nucleophilic protein GFP−Tag NLS ($F_n/F_c$ of 2.5, Figure 3B), supports the results obtained within transfected cells and confirms the nuclear accumulation of this truncated protein. Similarly, both FL MA and the 2−104 truncation exhibited the same pattern of nuclear exclusion observed in transfected cells (Figure 5A,C). Next we analyzed the localization of the nuclear-localizing $MA_{2-33}$ truncation in the absence of an intact nuclear envelope through the use of the detergent CHAPS. Nuclear accumulation of proteins in the absence of an intact nuclear envelope can only result from the interaction of the protein with a nuclear component-(s). For proteins such as the GFP−Tag NLS which do not bind to nuclear components, disruption of the nuclear envelope with CHAPS resulted in an even distribution of the protein between both the cytoplasm and the nucleus (Figure 5B,D, $F_n/F_c = 1$). Similarly, GFP alone is distributed evenly throughout the cell ($F_n/F_c = 1$) in either the absence or presence of an intact nuclear envelope (Figure 5B,E). In contrast, HIV-1 IN retains a significant degree of nuclear accumulation in the absence of an intact nuclear envelope due to its interaction with DNA (*41*) (Figure 5B,F, $F_n/F_c$ of 2 in the presence of CHAPS). $MA_{2-33}$−GFP also retained a similar level of nuclear accumulation in both the presence and absence of an intact nuclear envelope (Figure 5A,G, $F_n/F_c$ of 1.4 in both cases). This result suggests that the nuclear accumulation observed with the $MA_{2-33}$ truncation is likely due to interaction with a nuclear component rather than the result of facilitated nuclear import via the action of a genuine NLS.

*The N-Terminal Region of MA Interacts with DNA via a Process Requiring Residues $^{26}$KK.* Although $MA_{2-33}$ may be interacting with any number of nuclear components, the predominance of basic residues within this domain led us to test the possibility that it could be interacting with DNA. We therefore used DNA gel shift analysis to investigate the interaction of various GFP-tagged MA truncations with DNA. All GFP-tagged MA truncations containing the N-terminal basic domain (residues 2−33) were found to be

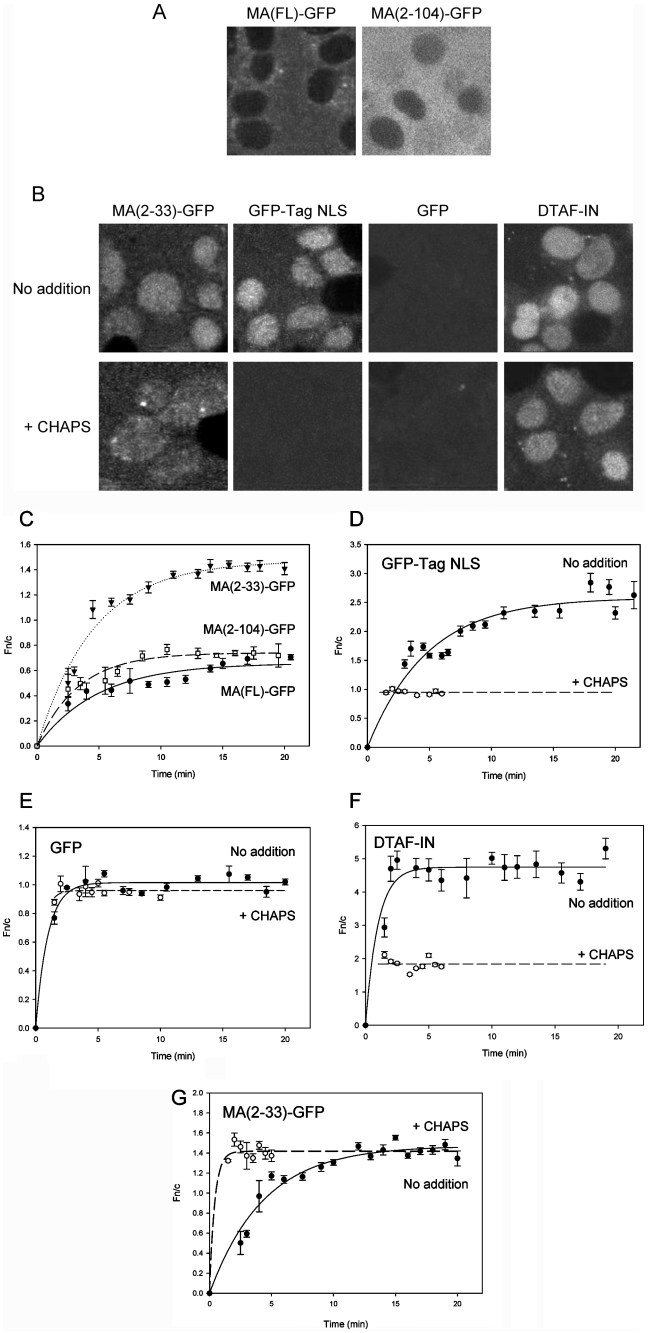


FIGURE 5: $MA_{2-33}$−GFP accumulates within the nucleus of semi-intact cells in vitro. The nuclear accumulation of GFP-tagged truncated MA proteins in the presence and absence of an intact nuclear envelope (induced by the addition of 0.025% CHAPS) was determined in vitro as described in the Materials and Methods. (A) Typical CLSM images of the cellular localization of $MA_{FL}$−GFP and $MA_{2-104}$−GFP. (B) Typical CLSM images of the cellular localization of $MA_{2-33}$−GFP together with control proteins GFP−Tag NLS, GFP, and DTAF-labeled IN protein in the presence (upper panels) and absence (lower panels) of an intact nuclear envelope. (C) Import kinetics for the nuclear accumulation of $MA_{FL}$−GFP (circles), $MA_{2-33}$−GFP (triangles), and $MA_{2-104}$−GFP (squares) into intact nuclei were determined from images such as those in (A) as described in the caption to Figure 2. Import kinetics for the nuclear accumulation of GFP−Tag NLS (D), GFP (E), DTAF−IN (F), and $MA_{2-33}$−GFP (G) in the absence (open circles) or presence (filled circles) of an intact nuclear envelope were determined as described in (B). The values represent the mean $F_n/F_c \pm$ SEM ($n \geq 5$) from a single representative experiment.

able to interact with DNA, as indicated by the retarded electrophoretic mobility of the DNA target (Figure 6A, upper panel). In contrast, GFP−$MA_{34-132}$, which lacks this region, exhibited a minimal interaction with DNA, supporting the notion that the interaction is primarily mediated by the N-terminal basic domain of MA. Importantly, the $^{26}$KK−TT mutation completely abolished the ability of all mutant MA protein derivatives to interact with DNA (Figure 6A, lower panels). Identical results were observed when a plasmid containing the HIV cDNA (pNL4-3) was used as the DNA target (data not shown). These results imply that the N-terminal basic region of MA interacts with both HIV-1-specific and -unrelated DNA via a mechanism which absolutely requires the $^{26}$KK residues.

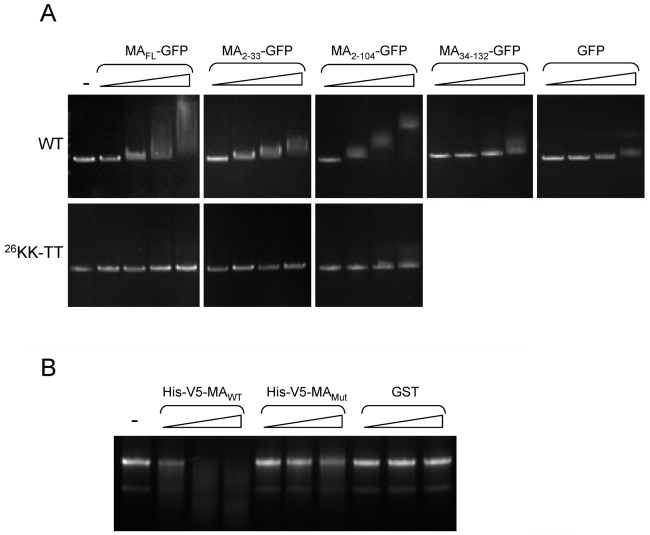


FIGURE 6: MA binds DNA and RNA via an interaction requiring the $^{26}$KK residues. (A) A 250 ng portion of linearized plasmid DNA was preincubated with increasing concentrations (1−8 $\mu$M) of recombinant GFP-tagged WT (upper panels) or $^{26}$KK−TT-mutant (lower panels) MA proteins or GFP alone as indicated, and the complexes were resolved on an 0.8% agarose gel. The DNA was visualized via ethidium bromide staining. A retardation of the electrophoretic ability of the DNA was taken as indicative of a positive binding interaction. (B) Total cellular RNA was extracted from HeLa cells and preincubated with 2, 4, or 8 $\mu$M His−V5-tagged WT or $^{26}$KK−TT-mutated MA protein (together with a GST control), and the complexes were resolved and visualized as described in (A).

During infection, the HIV PIC is formed either prior to or concurrent with the initiation of reverse transcription, meaning that the HIV genome may still be in an RNA form when proteins such as MA are incorporated into the complex. MA has been reported to interact with RNA also (*46*, *47*), so to determine whether the $^{26}$KK residues were also crucial for the ability of MA to bind RNA, a similar binding assay was performed using total cellular RNA. For these experiments, nonfluorescently tagged recombinant MA protein was used as GFP-tagged MA obscured the visibility of the RNA on an agarose gel. Figure 6B shows that $His_{6}$–V5 tagged MA exhibited a positive interaction with RNA within this assay (as indicated by the altered electrophoretic mobility of the RNA), while the $^{26}$KK−TT mutation abolished this interaction (Figure 6B). GST alone did not influence the electrophoretic mobility of RNA, suggesting that the altered appearance of RNA incubated with $MA_{WT}$ is indicative of a specific binding interaction. Although the nucleic acids used here were not HIV-specific, this assay indicates that MA has the ability to interact with both DNA and RNA via a

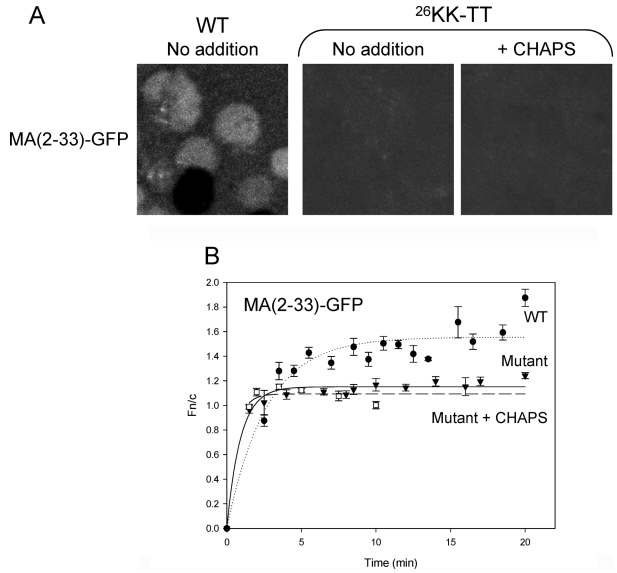


FIGURE 7: The $^{26}$KK−TT mutation reduces the nuclear retention of $MA_{2-33}$−GFP. The cellular localization of mutated $MA_{2-33}$−GFP protein was analyzed in vitro as described in the caption to Figure 3. (A) Typical CLSM images of the nuclear accumulation of $MA_{2-33}$−GFP containing a $^{26}$KK−TT mutation in the absence and presence of an intact nuclear envelope (induced by the addition of CHAPS) as indicated. An image of the WT protein is included for comparison. (B) Nuclear import kinetics of mutant $MA_{2-33}$−GFP in the presence (triangles) or absence (squares) of an intact nuclear envelope are shown. The kinetics for the import of the WT protein (circles) into intact nuclei are included for comparison.

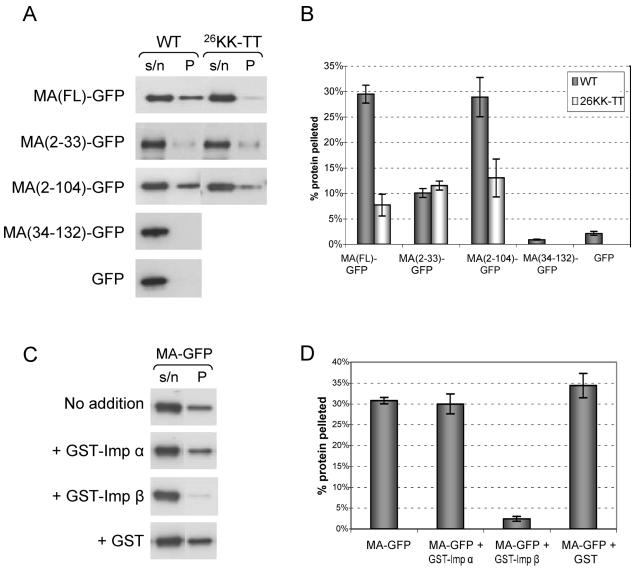


FIGURE 8: MA−GFP forms aggregates via a mechanism requiring the C-terminus of MA and the $^{26}$KK−TT residues which is inhibited by the addition of Imp $\beta$. (A) The degree of protein aggregation exhibited by WT and $^{26}$KK−TT-mutant GFP-tagged MA proteins was determined by sedimentation analysis. WT (left panels) and mutant (right panels) forms of GFP-tagged MA truncations, or GFP alone, were centrifuged at 100000*g* for 1 h, and the protein content of the supernatant (s/n) and pellet (P) fractions was determined by Western blotting. Similar results were observed following centrifugation at 150000*g* (data not shown). (B) Densitometric analysis was performed on Western blot films such as those in (A) using ImageJ software. The values represent the amount of protein pelleted (as a percentage of the total protein) ± SEM ($n \geq 3$). (C) $MA_{FL}$−GFP was preincubated with GST−Imp α, GST−Imp $\beta$, or GST alone prior to sedimentation and Western blot analysis as described in (A). (D) Densitometric analysis was performed on Western blot films such as those in (C) as described in (B).

mechanism which is dependent on the integrity of the $^{26}$KK residues.

*The $^{26}$KK−TT Mutation Reduces Nuclear Retention of $MA_{2-33}$−GFP in Vitro.* To determine the extent to which the DNA binding properties of MA contributed to the nuclear localization of the $MA_{2-33}$−GFP protein, an in vitro transport assay was utilized to assess the cellular localization of this mutant. As expected given the results of the DNA binding assay, the $^{26}$KK−TT mutation abolished the nuclear accumulation conferred by $MA_{2-33}$, in both the presence and absence of an intact nuclear envelope (Figure 7). These results suggest that the nuclear accumulation conferred by the N-terminal basic region of MA is most likely attributable to nuclear retention, potentially mediated by DNA binding.

*Aggregate Formation by MA Requires the $^{26}$KK Residues and Is Inhibited by Imp $\beta$.* Having determined that the likely basis of the nuclear accumulation conferred by $MA_{2-33}$ is through binding to nuclear components, we sought to investigate the mechanism responsible for the observed nuclear exclusion of the GFP-tagged $MA_{FL}$ and $MA_{2-104}$ constructs. While conducting unrelated experiments, we noted that high-speed (but not low-speed) centrifugation of MA−GFP protein resulted in pelleting of a considerable portion of the protein present. We postulated that MA had the potential to form high-order multimers/aggregates and that this may contribute to the inability of MA protein to freely diffuse into the nucleus of cells. MA is known to form trimers (*48*) and is also thought to form larger multimeric structures during viral assembly and within the mature HIV virion, where it forms a proteinaceous shell beneath the viral envelope (*49*). If this aggregative property of MA was responsible for the nuclear exclusion of $MA_{WT}$ observed both in vitro and in vivo, we hypothesized that this ability may be impaired in the $^{26}$KK−TT mutant, which was clearly able to freely diffuse throughout the cell (Figure 4B). To test this, we subjected both WT MA−GFP and the $^{26}$KK−TT-mutant derivative to high-speed centrifugation and determined the amount of aggregated protein able to sediment under these conditions using Western blot analysis. Figure 8A demonstrates that a substantial portion of WT MA−GFP protein was found within the pelleted fraction. In contrast, very little $^{26}$KK−TT-mutated MA−GFP protein was observed within the pelleted fraction, implying that protein aggregation was reduced. The lack of protein sedimentation observed for GFP alone confirmed the observed aggregation was due to the MA portion of the fusion protein. We extended this analysis to the truncated forms of MA and found that WT $MA_{2-104}$−GFP also exhibited protein aggregation which was markedly reduced by the $^{26}$KK−TT mutation. $MA_{2-33}$−GFP showed a reduced degree of protein aggregation, with very little difference observed between the WT and mutant forms, while almost no aggregation was seen with $MA_{34-132}$−GFP (Figure 8A,B). These results suggest that MA has a propensity to form large sedimenting structures and that the formation of these structures requires both the C-terminus and the $^{26}$KK residues. While these aggregates may indeed represent large multimers of MA, detailed structural analysis would be required to definitively confirm this.

Although MA exhibits a strong interaction with Imp $\beta$ (Figure 1), the inability of MA to target the nucleus within both in vivo and in vitro assays suggested that this complex

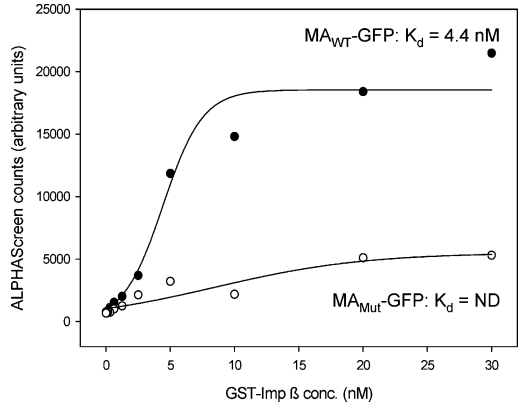


FIGURE 9: The $^{26}$KK−TT mutation impairs the ability of MA−GFP to interact with Imp $\beta$. The ability of both WT (filled circles) and $^{26}$KK−TT-mutated (open circles) MA−GFP protein to interact with Imp $\beta$ was assessed using an ALPHAScreen assay as described in the caption to Figure 1. Each point represents the average of triplicate results from a single representative experiment with the $K_d$ values indicated. ND = $K_d$ not able to be determined due to low binding.

may be nonproductive in terms of nuclear import. Aside from mediating nuclear import, Imp's such as Imp $\beta$ have been proposed to perform a chaperone function within the cell by binding to highly basic regions within proteins and preventing them from aggregating and precipitating (*50*). To determine whether the interaction of MA with Imp $\beta$ influences its ability to form aggregates, MA−GFP was preincubated with GST-tagged Imp α, Imp $\beta$, or GST alone prior to sedimentation. Figure 8C,D shows that substantially less MA−GFP protein was observed to sediment in the presence of Imp $\beta$, while preincubation of MA−GFP with either Imp α or GST alone had no such effect. Given the reduced propensity of the MA $^{26}$KK−TT mutant to form protein aggregates, we predicted that the ability of this protein to bind Imp $\beta$ may be similarly reduced. An ALPHAScreen assay was utilized to compare the binding of both WT and $^{26}$KK−TT-mutant MA−GFP protein to Imp $\beta$ and confirmed that this mutation does indeed exhibit a reduced interaction with Imp $\beta$ (Figure 9). These results indicate that MA binds to Imp $\beta$ via a mechanism involving the $^{26}$KK residues and that this interaction impairs the propensity of MA to form aggregates.

*Imp $\beta$ Inhibits the Interaction of MA with DNA.* Our results indicate that the interaction of MA with both Imp $\beta$ and DNA required the integrity of residues within the N-terminus, suggesting that Imp $\beta$ and DNA may bind to a similar region of MA. To determine whether Imp $\beta$ and DNA compete for the same binding site within MA, we performed a DNA gel shift assay in the presence of increasing concentrations of Imp $\beta$. Figure 10 shows that preincubating MA−GFP with increasing concentrations of GST-tagged Imp $\beta$ inhibits the ability of MA to bind DNA. GST alone had no such effect, confirming that the inhibition was specific to the Imp $\beta$ portion of the fusion protein. This suggests that Imp $\beta$ and DNA compete for a similar binding site within MA, of which $^{26}$KK are critical residues.

## DISCUSSION

Investigating the contribution of MA to the nuclear import of HIV cDNA has been complicated by the seemingly

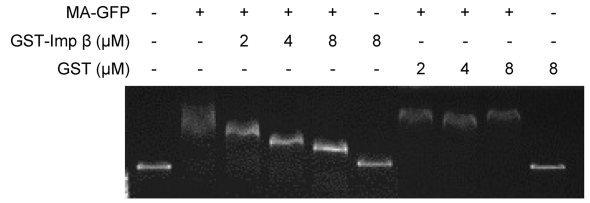


FIGURE 10: Imp $\beta$ impairs the ability of MA to interact with DNA. The ability of MA to interact with DNA in the presence of Imp $\beta$ was determined using a gel shift assay. MA−GFP (2 $\mu$M) was preincubated with increasing concentrations (2−8 $\mu$M) of either Imp $\beta$−GST or GST prior to the addition of 250 ng of linearized plasmid DNA. The DNA complexes were resolved on an agarose gel as described in the caption to Figure 6. Identical results were obtained when either a plasmid containing the HIV genome (pNL4-3) or an unrelated plasmid was used as the DNA target.

contradictory information regarding the nuclear import properties of this protein. The results obtained in this study may offer an explanation for the conflicting data regarding the cellular targeting properties of MA which exist within the literature. Through the use of truncated MA proteins, we determined that there are a number of important domains within MA which influence subcellular localization. The observed nuclear localization of the purported NLS-containing N-terminal region of MA is consistent with previous reports (*12*, *13*), but a more in depth analysis of the nucleophilic properties of the $MA_{2-33}$ protein using our in vitro nuclear transport assay suggested that the observed nuclear accumulation may not be due to the action of a conventional NLS; rather, this region appears to confer nuclear localization by facilitating binding to a nuclear component. Indeed, MA was found to interact with DNA via a mechanism dependent on the $^{26}$KK residues, and mutation of these residues abolished this interaction and reduced the nuclear accumulation conferred by $MA_{2-33}$ (see below).

In light of these results which suggest that full-length MA does not contain a conventional NLS, the finding that MA interacts strongly with Imp's was unexpected. While we did find an interaction between MA and the Imp α/$\beta$ heterodimer, we could not detect a strong interaction with Imp α alone. We also failed to detect an interaction between MA and other Imp α homologues including Npi1 and Qip1 (data not shown), suggesting this result is not limited to the version of Imp α (Rch1) used here. The observation that MA interacts with Imp $\beta$ is novel, and although Imp $\beta$ alone can mediate nuclear import of a number of cargoes (*51*−*53*), the inability of MA to enter the nucleus both in transfected cells and in our reconstituted *in vitro* system suggests that this interaction does not result in MA nuclear import. We note that the Imp binding properties of myristoylated MA may vary from those of the recombinant, unmyristoylated protein utilized within these experiments. However, our observation that the myristoylation-competent MA−V5 construct is also excluded from the nucleus of mammalian cells suggests that myristoylation alone does not result in the formation of a productive import complex. Imp $\beta$ is known to form import-defective complexes with proteins which contain highly basic regions including ribosomal proteins (*50*) and HIV IN (*41*), and this appears to be the case for MA as well. The binding of Imp $\beta$ to MA did, however, appear to reduce MA's ability to form aggregates, which supports the idea that Imp $\beta$ can function as a

chaperone for highly basic proteins (*50*). The formation of an import-defective complex between MA and Imp $\beta$ within the cell would preclude the passive diffusion of MA into the nucleus, also contributing to the nuclear exclusion of MA observed within this study. Whether the interaction of MA with Imp $\beta$ is relevant for HIV infection remains to be elucidated.

Given that all MA truncations containing an intact N-terminus can bind DNA, we were surprised to find these proteins excluded from the nucleus. Although the possibility of non-Crm1-mediated nuclear export cannot be excluded, the fact that GFP-tagged $MA_{34-132}$ is not excluded from the nucleus opposes the idea that MA contains an NES between residues 34 and 104. An alternative explanation for these findings is that the presence of an intact N-terminus results in the formation of large aggregates of MA, which prevents the free diffusion of this protein throughout the cell and acts to retain it in the cytoplasm. This idea is supported by the sedimentation analysis which revealed that both $MA_{FL}$−GFP and $MA_{2-104}$−GFP show a propensity to form large aggregates, while the $^{26}$KK−TT-mutant derivatives do not. This phenomenon correlates well with the nuclear exclusion of the WT but not the mutant forms of GFP-tagged $MA_{FL}$ and $MA_{2-104}$ observed both within transfected cells and in vitro. Additionally, the $MA_{2-33}$ and the $MA_{34-132}$ truncations, which do not exhibit nuclear exclusion, also do not possess a strong ability to form protein aggregates. The N-terminus of MA is crucial for its ability to trimerize and form multimers (*54*), and this multimerization is enhanced by the presence of downstream regions within the Gag polyprotein (*55*). During HIV infection, MA multimerization is essential for the ability of MA, and thus Gag, to bind the plasma membrane during assembly (*56*), and the results obtained here suggest that the $^{26}$KK residues, in addition to regions within aa's 34−104, may be important for this process. While far from conclusive, the differing aggregative abilities of the various MA truncations demonstrated here may contribute to the observed subcellular distribution of these proteins. Additionally, Imp's may play a role in coordinating the association and disassociation of MA monomers and thus influence the subcellular targeting of MA and MA-containing complexes throughout viral infection.

In addition to the effect on protein aggregation, mutation of the $^{26}$KK residues abolished the nuclear accumulation of GFP-tagged $MA_{2-33}$, most likely due to the effect of this mutation on the ability of MA to bind DNA. The DNA binding ability of all truncations was abolished by this mutation, as was the cytoplasmic retention of the FL and 2−104 fusion proteins. This mutation also abolished the ability of $MA_{FL}$ to interact with RNA. While it is not possible to exclude the possibility that this mutation results in an altered conformational state of MA, rendering it nonfunctional, the fact that these residues reside on an exposed loop of the protein's tertiary structure, as opposed to an internal buried site (see ref *54*) is not consistent with this idea. We believe that this region, comprising the protruding loop region between aa 18 and aa 31 (including two short $\beta$ sheet strands), is an important structural and functional domain which is crucial for a number of MA's properties, including DNA/RNA binding and protein multimerization. Indeed, this region has been shown to interact with HIV RNA (*57*) and is known to be required for the interaction of MA with the plasma membrane (*58*). Results presented within this study showed that Imp $\beta$ competes with DNA for MA binding and also that mutation of the $^{26}$KK residues markedly impairs the ability of MA to interact with Imp $\beta$. Taken together, these results suggest that the N-terminal region of MA also contains the Imp $\beta$ binding site. It is clear that this region of MA is capable of interacting with a number of cellular components including Imp $\beta$, DNA/RNA, and the plasma membrane. Whether these interactions play a role during the course of HIV infection and, if so, how these competing interactions are regulated is an area which warrants further investigation.

The effect of mutations within the N-terminal basic region of MA on virus infectivity in vivo has been studied extensively by others (*18*, *20*, *21*) and supports the requirement of this region of MA for maximum viral infectivity. While it is known that this mutation has a negative impact on infectivity, the nature of this impairment remains controversial. The results obtained within this study support the theory that MA is unlikely to be involved in PIC nuclear import, suggesting that the observed infectivity defects are due to the impact of these mutations on other functions of MA. MA is capable of binding to and recruiting the HIV RNA genome into assembling viruses (*47*), and the impact of basic-domain mutations on the RNA binding ability of MA demonstrated here may affect this process and may thus impair the production of infectious virions. The DNA/RNA binding ability conferred by the basic domain of MA may also be important for the incorporation of MA into the PIC, where it may serve a non-import-related role such as protection of the genome, recruitment of required cellular components, or aiding the passage of the PIC through the cellular cytoplasm. The potential roles of MA discussed above assume that the properties of PIC-associated MA are similar to those of the isolated protein examined here, but further work will be required to confirm that this is the case. Our finding that the $^{26}$KK residues are also important for MA aggregation suggests that mutations within this region may affect MA multimerization in vivo and thus impair the MA-mediated process of plasma membrane binding and HIV assembly. Investigating the ultrastructure of virions containing $^{26}$KK−TT-mutated MA would shed more light on this possibility.

The discovery that the N-terminal basic domain of MA is such a fundamental structural determinant of many of MA's functions including DNA/RNA binding and high-order protein multimerization highlights the enormous potential of this region as a therapeutic target.

## ACKNOWLEDGMENT

We thank Judy Edmonds for technical assistance. The following reagents were obtained through the AIDS Research and Reference Reagent Program, Division of AIDS, NIAID, NIH: antiserum to p17 from Dr. Paul Spearman; pNL4-3 from Dr. Malcolm Martin.

## REFERENCES

1. Freed, E. O. (2001) HIV-1 replication, *Somatic Cell Mol. Genet. 26*, 13−33.
2. Bukrinsky, M. I., Sharova, N., McDonald, T. L., Pushkarskaya, T., Tarpley, W. G., and Stevenson, M. (1993) Association of integrase, matrix, and reverse transcriptase antigens of human

immunodeficiency virus type 1 with viral nucleic acids following acute infection, *Proc. Natl. Acad. Sci. U.S.A. 90*, 6125−6129.
3. Fassati, A., and Goff, S. P. (2001) Characterization of intracellular reverse transcription complexes of human immunodeficiency virus type 1, *J. Virol. 75*, 3626−3635.
4. Weinberg, J. B., Matthews, T. J., Cullen, B. R., and Malim, M. H. (1991) Productive human immunodeficiency virus type 1 (HIV-1) infection of nonproliferating human monocytes, *J. Exp. Med. 174*, 1477−1482.
5. Bukrinsky, M. (2004) A hard way to the nucleus, *Mol. Med. 10*, 1−5.
6. Stewart, M., Baker, R. P., Bayliss, R., Clayton, L., Grant, R. P., Littlewood, T., and Matsuura, Y. (2001) Molecular mechanism of translocation through nuclear pore complexes during nuclear protein import, *FEBS Lett. 498*, 145−149.
7. Macara, I. G. (2001) Transport into and out of the nucleus, *Microbiol. Mol. Biol. Rev. 65*, 570−594, Table of Contents.
8. Steggerda, S. M., and Paschal, B. M. (2002) Regulation of nuclear import and export by the GTPase Ran, *Int. Rev. Cytol. 217*, 41−91.
9. Pemberton, L. F., and Paschal, B. M. (2005) Mechanisms of receptor-mediated nuclear import and nuclear export, *Traffic 6*, 187−198.
10. Piller, S. C., Caly, L., and Jans, D. A. (2003) Nuclear import of the pre-integration complex (PIC): the Achilles heel of HIV? *Curr. Drug Targets 4*, 409−429.
11. Yamashita, M., and Emerman, M. (2006) Retroviral infection of non-dividing cells: old and new perspectives, *Virology 344*, 88−93.
12. Bukrinsky, M. I., Haggerty, S., Dempsey, M. P., Sharova, N., Adzhubel, A., Spitz, L., Lewis, P., Goldfarb, D., Emerman, M., and Stevenson, M. (1993) A nuclear localization signal within HIV-1 matrix protein that governs infection of non-dividing cells [see comment], *Nature 365*, 666−669.
13. Haffar, O. K., Popov, S., Dubrovsky, L., Agostini, I., Tang, H., Pushkarsky, T., Nadler, S. G., and Bukrinsky, M. (2000) Two nuclear localization signals in the HIV-1 matrix protein regulate nuclear import of the HIV-1 pre-integration complex, *J. Mol. Biol. 299*, 359−368.
14. Gallay, P., Stitt, V., Mundy, C., Oettinger, M., and Trono, D. (1996) Role of the karyopherin pathway in human immunodeficiency virus type 1 nuclear import, *J. Virol. 70*, 1027−1032.
15. Nadler, S. G., Tritschler, D., Haffar, O. K., Blake, J., Bruce, A. G., and Cleaveland, J. S. (1997) Differential expression and sequence-specific interaction of karyopherin alpha with nuclear localization sequences, *J. Biol. Chem. 272*, 4310−4315.
16. von Schwedler, U., Kornbluth, R. S., and Trono, D. (1994) The nuclear localization signal of the matrix protein of human immunodeficiency virus type 1 allows the establishment of infection in macrophages and quiescent T lymphocytes, *Proc. Natl. Acad. Sci. U.S.A. 91*, 6992−6996.
17. Freed, E. O., and Martin, M. A. (1994) HIV-1 infection of non-dividing cells, *Nature 369*, 107−108.
18. Fouchier, R. A., Meyer, B. E., Simon, J. H., Fischer, U., and Malim, M. H. (1997) HIV-1 infection of non-dividing cells: evidence that the amino-terminal basic region of the viral matrix protein is important for Gag processing but not for post-entry nuclear import, *EMBO J. 16*, 4531−4539.
19. Kootstra, N. A., and Schuitemaker, H. (1999) Phenotype of HIV-1 lacking a functional nuclear localization signal in matrix protein of gag and Vpr is comparable to wild-type HIV-1 in primary macrophages, *Virology 253*, 170−180.
20. Mannioui, A., Nelson, E., Schiffer, C., Felix, N., Le Rouzic, E., Benichou, S., Gluckman, J. C., and Canque, B. (2005) Human immunodeficiency virus type 1 KK26−27 matrix mutants display impaired infectivity, circularization and integration but not nuclear import, *Virology 339*, 21−30.
21. Reil, H., Bukovsky, A. A., Gelderblom, H. R., and Gottlinger, H. G. (1998) Efficient HIV-1 replication can occur in the absence of the viral matrix protein, *EMBO J. 17*, 2699−2708.
22. Lu, R., Limon, A., Devroe, E., Silver, P. A., Cherepanov, P., and Engelman, A. (2004) Class II integrase mutants with changes in putative nuclear localization signals are primarily blocked at a postnuclear entry step of human immunodeficiency virus type 1 replication, *J. Virol. 78*, 12735−12746.
23. Petit, C., Schwartz, O., and Mammano, F. (2000) The karyophilic properties of human immunodeficiency virus type 1 integrase are not required for nuclear import of proviral DNA, *J. Virol. 74*, 7119−7126.
24. Dvorin, J. D., Bell, P., Maul, G. G., Yamashita, M., Emerman, M., and Malim, M. H. (2002) Reassessment of the roles of integrase and the central DNA flap in human immunodeficiency virus type 1 nuclear import, *J. Virol. 76*, 12087−12096.
25. Limon, A., Nakajima, N., Lu, R., Ghory, H. Z., and Engelman, A. (2002) Wild-type levels of nuclear localization and human immunodeficiency virus type 1 replication in the absence of the central DNA flap, *J. Virol. 76*, 12078−12086.
26. Arhel, N. J., Souquere-Besse, S., Munier, S., Souque, P., Guadagnini, S., Rutherford, S., Prevost, M. C., Allen, T. D., and Charneau, P. (2007) HIV-1 DNA Flap formation promotes uncoating of the pre-integration complex at the nuclear pore, *EMBO J. 26*, 3025−3037.
27. Yamashita, M., and Emerman, M. (2005) The cell cycle independence of HIV infections is not determined by known karyophilic viral elements, *PLoS Pathog. 1*, e18.
28. Yu, G., Shen, F. S., Sturch, S., Aquino, A., Glazer, R. I., and Felsted, R. L. (1995) Regulation of HIV-1 gag protein subcellular targeting by protein kinase C, *J. Biol. Chem. 270*, 4792−4796.
29. Depienne, C., Roques, P., Creminon, C., Fritsch, L., Casseron, R., Dormont, D., Dargemont, C., and Benichou, S. (2000) Cellular distribution and karyophilic properties of matrix, integrase, and Vpr proteins from the human and simian immunodeficiency viruses, *Exp. Cell Res. 260*, 387−395.
30. Dupont, S., Sharova, N., DeHoratius, C., Virbasius, C. M., Zhu, X., Bukrinskaya, A. G., Stevenson, M., and Green, M. R. (1999) A novel nuclear export activity in HIV-1 matrix protein required for viral replication, *Nature 402*, 681−685.
31. Hearps, A. C., and Jans, D. A. (2007) Regulating the functions of the HIV-1 matrix protein, *AIDS Res. Hum. Retroviruses 23*, 341−346.
32. Freed, E. O., Englund, G., and Martin, M. A. (1995) Role of the basic domain of human immunodeficiency virus type 1 matrix in macrophage infection, *J. Virol. 69*, 3949−3954.
33. Yu, X., Yuan, X., Matsuda, Z., Lee, T. H., and Essex, M. (1992) The matrix protein of human immunodeficiency virus type 1 is required for incorporation of viral envelope protein into mature virions, *J. Virol. 66*, 4966−4971.
34. Spearman, P., Wang, J. J., Vander, Heyden, N., and Ratner, L. (1994) Identification of human immunodeficiency virus type 1 Gag protein domains essential to membrane binding and particle assembly, *J. Virol. 68*, 3232−3242.
35. Yuan, X., Yu, X., Lee, T. H., and Essex, M. (1993) Mutations in the N-terminal region of human immunodeficiency virus type 1 matrix protein block intracellular transport of the Gag precursor, *J. Virol. 67*, 6387−6394.
36. Casella, C. R., Raffini, L. J., and Panganiban, A. T. (1997) Pleiotropic mutations in the HIV-1 matrix protein that affect diverse steps in replication, *Virology 228*, 294−306.
37. Ghildyal, R., Ho, A., Wagstaff, K. M., Dias, M. M., Barton, C. L., Jans, P., Bardin, P., and Jans, D. A. (2005) Nuclear import of the respiratory syncytial virus matrix protein is mediated by importin beta1 independent of importin alpha, *Biochemistry 44*, 12887−12895.
38. Henderson, B. R., and Eleftheriou, A. (2000) A comparison of the activity, sequence specificity, and CRM1-dependence of different nuclear export signals, *Exp. Cell Res. 256*, 213−224.
39. Hubner, S., Xiao, C. Y., and Jans, D. A. (1997) The protein kinase CK2 site (Ser111/112) enhances recognition of the simian virus 40 large T-antigen nuclear localization sequence by importin, *J. Biol. Chem. 272*, 17191−17195.
40. Baliga, B. C., Colussi, P. A., Read, S. H., Dias, M. M., Jans, D. A., and Kumar, S. (2003) Role of prodomain in importin-mediated nuclear localization and activation of caspase-2, *J. Biol. Chem. 278*, 4899−4905.
41. Hearps, A. C., and Jans, D. A. (2006) HIV-1 integrase is capable of targeting DNA to the nucleus via an importin alpha/beta-dependent mechanism, *Biochem. J. 398*, 475−484.
42. Jans, D. A., Jans, P., Briggs, L. J., Sutton, V., and Trapani, J. A. (1996) Nuclear transport of granzyme B (fragmentin-2). Dependence of perforin in vivo and cytosolic factors in vitro, *J. Biol. Chem. 271*, 30781−30789.
43. Efthymiadis, A., Briggs, L. J., and Jans, D. A. (1998) The HIV-1 Tat nuclear localization sequence confers novel nuclear import properties, *J. Biol. Chem. 273*, 1623−1628.
44. Wagstaff, K. M., and Jans, D. A. (2006) Intramolecular masking of nuclear localization signals: analysis of importin binding using a novel AlphaScreen-based method, *Anal. Biochem. 348*, 49−56.

45. Fischer, U., Huber, J., Boelens, W. C., Mattaj, I. W., and Luhrmann, R. (1995) The HIV-1 Rev activation domain is a nuclear export signal that accesses an export pathway used by specific cellular RNAs, *Cell 82*, 475−483.
46. Lochrie, M. A., Waugh, S., Pratt, D. G., Jr., Clever, J., Parslow, T. G., and Polisky, B. (1997) In vitro selection of RNAs that bind to the human immunodeficiency virus type-1 gag polyprotein, *Nucleic Acids Res. 25*, 2902−2910.
47. Ott, D. E., Coren, L. V., and Gagliardi, T. D. (2005) Redundant roles for nucleocapsid and matrix RNA-binding sequences in human immunodeficiency virus type 1 assembly, *J. Virol. 79*, 13839−13847.
48. Massiah, M. A., Worthylake, D., Christensen, A. M., Sundquist, W. I., Hill, C. P., and Summers, M. F. (1996) Comparison of the NMR and X-ray structures of the HIV-1 matrix protein: evidence for conformational changes during viral assembly, *Protein Sci. 5*, 2391−2398.
49. Gelderblom, H. R., Hausmann, E. H., Ozel, M., Pauli, G., and Koch, M. A. (1987) Fine structure of human immunodeficiency virus (HIV) and immunolocalization of structural proteins, *Virology 156*, 171−176.
50. Jakel, S., Mingot, J. M., Schwarzmaier, P., Hartmann, E., and Gorlich, D. (2002) Importins fulfil a dual function as nuclear import receptors and cytoplasmic chaperones for exposed basic domains, *EMBO J. 21*, 377−386.
51. Forwood, J. K., Harley, V., and Jans, D. A. (2001) The C-terminal nuclear localization signal of the sex-determining region Y (SRY) high mobility group domain mediates nuclear import through importin beta 1, *J. Biol. Chem. 276*, 46575−46582.
52. Lam, M. H., Briggs, L. J., Hu, W., Martin, T. J., Gillespie, M. T., and Jans, D. A. (1999) Importin beta recognizes parathyroid hormone-related protein with high affinity and mediates its nuclear import in the absence of importin alpha, *J. Biol. Chem. 274*, 7391−7398.
53. Truant, R., and Cullen, B. R. (1999) The arginine-rich domains present in human immunodeficiency virus type 1 Tat and Rev function as direct importin beta-dependent nuclear localization signals, *Mol. Cell. Biol. 19*, 1210−1217.
54. Massiah, M. A., Starich, M. R., Paschall, C., Summers, M. F., Christensen, A. M., and Sundquist, W. I. (1994) Three-dimensional structure of the human immunodeficiency virus type 1 matrix protein, *J. Mol. Biol. 244*, 198−223.
55. Burniston, M. T., Cimarelli, A., Colgan, J., Curtis, S. P., and Luban, J. (1999) Human immunodeficiency virus type 1 Gag polyprotein multimerization requires the nucleocapsid domain and RNA and is promoted by the capsid-dimer interface and the basic region of matrix protein, *J. Virol. 73*, 8527−8540.
56. Hill, C. P., Worthylake, D., Bancroft, D. P., Christensen, A. M., and Sundquist, W. I. (1996) Crystal structures of the trimeric human immunodeficiency virus type 1 matrix protein: implications for membrane association and assembly, *Proc. Natl. Acad. Sci. U.S.A. 93*, 3099−3104.
57. Purohit, P., Dupont, S., Stevenson, M., and Green, M. R. (2001) Sequence-specific interaction between HIV-1 matrix protein and viral genomic RNA revealed by in vitro genetic selection, *RNA 7*, 576−584.
58. Murray, P. S., Li, Z., Wang, J., Tang, C. L., Honig, B., and Murray, D. (2005) Retroviral matrix domains share electrostatic homology: models for membrane binding function throughout the viral life cycle, *Structure 13*, 1521−1531.

BI701360J